Wave overtopping layer thickness on the crest of rubble mound seawalls

Koosheh, Ali; Etemad-Shahidi, Amir; Cartwright, Nick; Tomlinson, Rodger; van Gent, Marcel R.A.

DOI
10.1016/j.coastaleng.2023.104441

Publication date
2023

Document Version
Final published version

Published in
Coastal Engineering

Coastal Engineering 188 (2024) 104441

Contents lists available at ScienceDirect

Coastal Engineering

journal homepage: www.elsevier.com/locate/coastaleng

Wave overtopping layer thickness on the crest of rubble mound seawalls

Ali Koosheh [a,*], Amir Etemad-Shahidi [a,b], Nick Cartwright [a], Rodger Tomlinson [c], Marcel R.A. van Gent [d,e]

[a] School of Engineering and Built Environment, Griffith University, Southport, QLD, 4222, Australia
[b] School of Engineering, Edith Cowan University, WA, 6027, Australia
[c] Coastal and Marine Research Centre, Griffith University, Southport, QLD, 4222, Australia
[d] Department of Coastal Structures & Waves, Deltares, 2600, MH, Delft, the Netherlands
[e] Department of Hydraulic Engineering, Delft University of Technology, 2628, CN, Delft, the Netherlands

ARTICLE INFO

Keywords:
Wave overtopping
Overtopping layer thickness
Rubble mound seawalls

ABSTRACT

During storms, ensuring the protection of people, vehicles and infrastructure on the crest of coastal structures from wave overtopping hazards is crucial. The thickness of the wave overtopping layer is a key variable used for assessing safety and maintaining a secure design. Traditionally, this parameter is associated with the height difference between the fictitious wave run-up level exceeded by 2% of waves and the crest freeboard of coastal structures. This study aims to investigate the wave overtopping layer thickness on the crest of rubble mound seawalls. To achieve this, a series of 125 small-scale 2D physical model tests were conducted on a two-layer rubble mound seawall with an impermeable core and slopes of 1:1.5 and 1:2. The obtained results indicated that the existing empirical formulas, originally developed for dikes, underestimate the overtopping layer thickness on the studied seawall. Therefore, modifications were made to the formulas found in the literature specifically tailored for rubble mound seawalls. The newly proposed formulas for estimating overtopping layer thickness at both the seaward edge and the middle of the crest showed improvements compared to the existing formulas.

1. Introduction

Rubble mound seawalls are constructed along coastlines to protect inland areas and infrastructure from wave attacks and coastal flooding. However, in situations where restricting public access to the structure's crest (e. g. a promenade) during a storm event is complicated or not feasible, wave overtopping can pose a significant threat to people and vehicles. Over the past few decades, there have been several reported fatal accidents caused by wave overtopping at or behind coastal protection structures (Allsop et al., 2003). Moreover, excessive wave overtopping can lead to structural failure. Coastal managers and engineers do not tend to build seawalls too high because of their high construction costs and visual impacts. On the other hand, due to sea level rise associated with climate change, more severe wave overtopping conditions are expected in the future. Therefore, conducting reliable risk assessments of coastal areas and implementing proper seawall designs are crucial to ensure adequate protection of communities and infrastructure.

A safe and cost-effective design of a seawall requires wave overtopping responses to be below specified allowable values (e.g., in design manuals). Accurately estimating overtopping characteristics is crucial for evaluating the extent of wave overtopping risks at coastal structures. This estimation can be achieved using empirical formulas derived from laboratory measurements based on influential structural and wave parameters. Historically, the mean wave overtopping rate q (l/s per m) has been the most commonly adopted parameter for studying overtopping hazards. Several studies have focused on estimating the overtopping discharge q for rubble mound seawalls (van Gent et al., 2007; Jafari and Etemad-Shahidi, 2011; van der Meer and Bruce, 2014; Etemad-Shahidi et al., 2022; Koosheh et al., 2020, 2022a). However, relying solely on average overtopping parameters is not sufficient as the highest risks of damage are associated with large overtopping events (see Koosheh et al., 2021, for a detailed overview of literature). Consequently, the maximum individual overtopping volume (V_{max}) was subsequently included in the definition of tolerable conditions (EurOtop, 2018). Estimating V_{max} requires statistical analysis of the distribution of individual overtopping

* Corresponding author.
E-mail address: ali.koosheh@griffithuni.edu.au (A. Koosheh).

https://doi.org/10.1016/j.coastaleng.2023.104441
Received 20 September 2023; Received in revised form 7 November 2023; Accepted 2 December 2023
Available online 8 December 2023

volumes (van der Meer and Janssen, 1994; Nørgaard et al., 2013; Zanuttigh et al., 2013; Mares-Nasarre et al., 2020). Recently, Koosheh et al. (2022b) conducted a comprehensive wave-by-wave study of overtopping at rubble mound seawalls and provided improved formulas for estimating V_{max}.

There is a knowledge gap regarding the criteria for human instability against overtopping flow. Even if overtopping volumes are below the tolerable threshold, there is no guarantee that overtopping flow will not pose a threat to people standing on the crest (Koosheh et al., 2021). Several studies have focused on the stability of humans against flood flow, introducing hydraulic parameters such as depth or velocity as criteria for stability (e.g., Foster and Cox, 1973; Abt et al., 1989; Jonkman and Penning-Rowsell, 2008; Arrighi et al., 2017). However, these studies, based on real-human experiments under steady flow conditions, are fundamentally different from wave overtopping, which involves highly transient flow. As a result, safety guidelines derived from flood studies cannot be directly applied to wave overtopping events (Cao et al., 2021). To establish reliable tolerable thresholds for wave overtopping events, a large dataset covering different structural features and wave conditions is necessary. The existing studies on human stability against overtopping flow are limited, and only a few works in the literature have investigated tolerable thresholds for overtopping flow parameters such as thickness or velocity (e.g., Takahashi et al., 1992; Endoh and Takahashi, 1994; Bae et al., 2016; Sandoval and Bruce, 2017).

As mentioned, the overtopping layer thickness (or flow depth) is a commonly used parameter for assessing human stability on the crest of coastal structures. This parameter varies temporally and spatially over the structure and can be studied from different perspectives depending on the project's purpose and importance. Initially, Cox and Machemehl (1986) proposed a theoretical-based formula for the evolution of the overtopping layer thickness over the crest. Subsequently, a series of studies (e.g., Schüttrumpf, 2001; van Gent, 2002; Schüttrumpf and van Gent, 2003) linked the thickness of the overtopping flow to the difference between the fictitious wave run-up on the seaward slope and the crest freeboard of dikes, utilizing empirical coefficients. More recently, Mares-Nasarre et al. (2019) adapted and calibrated existing formulas for mound breakwaters with a permeable core.

To the best of the authors' knowledge, no specific formula is currently available to estimate the wave overtopping layer thickness on the crest of rubble mound seawalls with an impermeable core. Existing formulas developed for other structures, such as dikes (smooth and impermeable) or breakwaters (rough and permeable), may not provide reliable estimations or have not been validated for rubble mound seawalls with an impermeable core. Therefore, the objective of this study is to investigate the overtopping layer thickness on rubble mound seawalls through 2D small-scale physical model tests. Additionally, the existing formulas derived from tests on other types of structures (e.g., dikes) are evaluated and modified based on the new dataset obtained from seawall overtopping experiments. The structure of the paper is organized as follows: Section 2 provides an overview of the existing formulas found in the literature. The experimental methodology and data analysis techniques are discussed in Sections 3 and 4, respectively. Section 5 presents the results of the analysis and the corresponding discussions. Finally, Section 6 summarizes the findings of this research.

2. Background

Schüttrumpf (2001) and van Gent (2002) conducted separate studies on the wave overtopping process on the crest and the landward slope of dikes. Schüttrumpf and van Gent (2003) integrated the results of the mentioned studies and correlated the overtopping layer thickness with a fictitious wave run-up height on a non-overtopped dike using a transfer function (see Fig. 1).

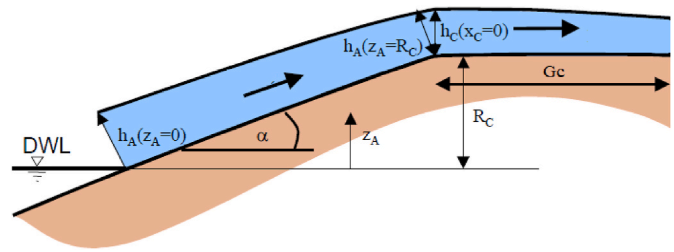

Fig. 1. Definition of overtopping flow layer profile by Schüttrumpf and van Gent (2003).

$$\frac{h_{A,2\%}(R_c)}{H_{m0}} = c^*_{A,h}\left(\frac{R_{u2\%} - R_c}{\gamma_f H_{m0}}\right) \tag{1}$$

where $h_{A,2\%}(R_c)$ is the overtopping layer thickness at the transition of seaward slope and crest (hereafter seaward edge) exceeded by 2% of incident waves, R_c is crest freeboard, H_{m0} is spectral significant wave height and $c^*_{A,h}$ is an empirical coefficient. Here, $R_{u2\%}$ stands for the wave run-up exceeded by 2% of incident waves and γ_f is a reduction factor that accounts for the roughness of the structure.

The second transfer function was defined to describe the evolution of overtopping layer thickness along the crest:

$$h_{c,2\%}(x_c) = h_{A,2\%}(R_c).\exp\left(-c^*_{c,h}\frac{x_c}{G_c}\right) \tag{2}$$

$h_{c,2\%}$ (x_c) is overtopping layer thickness on the crest, x_c is the distance from the seaward edge, G_c is the crest width, and $c^*_{c,h}$ is an empirical coefficient.

To estimate wave run-up exceeded by 2% of incident waves, Schüttrumpf and van Gent (2003) suggested the formula proposed by van Gent (2002) as follows:

$$\frac{R_{u2\%}}{\gamma_f H_{m0}} = c_0\, Ir_{m-1,0} \text{ if } Ir_{m-1,0} \le p \tag{3}$$

$$\frac{R_{u2\%}}{\gamma_f H_{m0}} = c_1 - \frac{c_2}{Ir_{m-1,0}} \text{ if } Ir_{m-1,0} > p$$

where $c_0 = 1.45$, $c_1 = 3.8$ and $Ir_{m-1,0}$ is Iribarren number (breaker parameter) defined as $\tan\alpha/\sqrt{(H_{m0}/L_{m-1,0})}$ where $L_{m-1,0} = (g/2\pi)\, T_{m-1,0}^2$. Parameters c_2 and p can be obtained based on c_0 and c_1 as:

$$c_2 = 0.25\frac{c_1^2}{c_0} \tag{4}$$

$$p = 0.5\frac{c_1}{c_0} \tag{5}$$

The coefficients proposed by Schüttrumpf (2001) and van Gent (2002) are compared in Table 1. However, there is a significant difference between the coefficients of these two studies, although the range of applicability of coefficients by van Gent (2002) falls within those proposed by Schüttrumpf (2001) in terms of the seaward slope. In summary, the coefficients from Schüttrumpf (2001) result in higher estimates of the overtopping layer thickness on dikes. While some authors have suggested that the empirical coefficients $c^*_{A,h}$ and $c^*_{c,h}$ depend on the seaward slope, further investigations are needed to gain a better understanding of the underlying physics of the problem (see Bosman, 2007). Van der Meer et al. (2010) proposed to use $c^*_{A,h} = 0.13$, which is close to 0.15 proposed by van Gent (2002).

To estimate overtopping layer thickness at the seaward edge of dikes, $h_{A,2\%}(R_c)$, EurOtop (2018) suggested Eq. (6) using $c^*_{A,h} = 0.2$ for the slopes of 1:3 and 4, and $c^*_{A,h} = 0.3$ for the slope of 1:6.

Table 1
Proposed empirical coefficients by different studies.

Study	$c^*_{A,h}$	$c^*_{c,h}$	Structure type	Slope	γ_f	Crest
van Gent (2002)	0.15	0.4	Dike	1:4	1	Smooth, Impermeable
Schüttrumpf (2001)	0.33	0.89	Dike	1:3, 1:4, 1:6	1	Smooth, Impermeable
van der Meer et al. (2010)	0.13	–	Dike	1:3	1	Smooth, Impermeable
EurOtop (2018)	0.2	a	Dike	1:3, 1:4	1	Smooth, Impermeable
	0.3			1:6		
Mares-Nasarre et al. (2019)	0.52	0.89	Rubble mound breakwater	1:1.5	0.4,0.47,0.49	Rough, Permeable

[a] Constant layer thickness along the crest.

$$\frac{h_{A,2\%}(R_c)}{H_{m0}} = c^*_{A,h}\left(\frac{R_{u2\%} - R_c}{H_{m0}}\right) \tag{6}$$

Wave run-up on the slope of the structure can be estimated as follows (TAW, 2002):

$$\frac{R_{u2\%}}{H_{m0}} = 1.65\,\gamma_f\,\gamma_\beta\,Ir_{m-1,0} \leq\ 1.0\,\gamma_\beta\left(4.0 - \frac{1.5}{\sqrt{Ir_{m-1,0}}}\right) \tag{7}$$

The parameter γ_β, as a reduction factor, accounts for the effects of wave obliquity. Based on the assumption that the overtopping layer thickness decreases abruptly behind the seaward edge of the crest and remains almost constant along the crest, EurOtop (2018) suggested the following equation:

$$h_{c,2\%}(x_c) = \frac{2}{3}\,h_{A,2\%}(R_c) \tag{8}$$

Chen et al. (2022) conducted a validation of a numerical model and analysed the differences between Eq. (1) and Eq. (6) with respect to the presence of the influence of the roughness (γ_f) of the seaward side in the righthand side of the equation, and concluded that this influence of the roughness (γ_f) as shown in Eq. (1) should be present, both based on physical reasoning and on variations of the roughness in the model. For smooth impermeable dikes for which there is limited roughness, this difference is not essential but for structures like the one examined here, this difference is important.

Mares-Nasarre et al. (2019) conducted small-scale physical tests on breakwaters (slope: 1:1.5) with different armour layers. They showed that Eqs. (2) and (6), using the existing empirical coefficients for dikes, do not lead to a good estimation of wave overtopping layer thickness on rubble mound breakwaters. The authors used Eq. (9), proposed by TAW (2002), for rubble mound structures, to estimate wave run-up and proposed to use $c^*_{A,h} = 0.52$ and $c^*_{c,h} = 0.89$ in Eqs. (6) and (2) respectively.

$$\frac{R_{u2\%}}{H_{m0}} = 1.65\,\gamma_f\,\gamma_\beta\,Ir_{m-1,0} \leq 1.0\,\gamma_{f\ surging}\,\gamma_\beta\left(4.0 - \frac{1.5}{\sqrt{Ir_{m-1,0}}}\right) \tag{9}$$

where

$$\gamma_{f\ surging} = \gamma_f + \frac{(Ir_{m-1,0} - 1.8)(1 - \gamma_f)}{8.2} \tag{10}$$

with a maximum of $R_{u2\%}/H_{m0} = 2.0$ (3.0) for structures with a permeable (impermeable) core. Table 1 summarizes the empirical coefficients proposed by different authors. It is evident that larger empirical coefficients are suggested for rubble mound structures compared to dikes. The difference in coefficients obtained for the given structure types can be attributed to their structural features. The slope angle and roughness, the crest's roughness, and the permeability of the core are the governing factors that can affect wave run-up on the slope and the formation of the overtopping flow over the crest.

Dikes are impermeable structures with a smooth slope where $\gamma_f = 1$ is recommended in the literature. On the other hand, rubble mound structures such as breakwaters and seawalls have a rough surface that plays an important role in the interaction between the structure and incident waves. The roughness factor of these structures varies between 0.38 and 0.60, depending on the armour layer type, the number of layers, and core permeability. The main difference between rubble mound breakwaters and seawalls is their permeability. Breakwaters commonly have a permeable core, while seawalls mostly have an impermeable core and have a slightly higher γ_f compared to breakwaters.

3. Physical model tests

3.1. Experimental set up

Small-scale physical model tests were conducted in the wave flume of the hydraulic laboratory at Griffith University, Australia (Fig. 2). The wave flume is 0.5 m wide, 22.5 m long, and 0.8 m deep and is equipped with a piston-type wave maker. To prevent re-reflection of waves from the paddle, reflected waves from the structure were absorbed using a dynamic absorption system. To estimate incident wave parameters near the structure's toe, three wave gauges were used to measure the water free surface elevations, and the method proposed by Mansard and Funke (1980) was employed to separate incident and reflected waves. Regular checks were performed on the still water level and probe calibration to ensure measurement accuracy during the experiments. In order to prevent any potential impacts of overtopped volume of water, natural evaporation, and facility leakages, the water surface level in the flume was consistently monitored. In addition, the calibration of wave gauges was checked daily to ensure the accuracy of water free surface reading.

As depicted in Fig. 2, the tests were conducted on a 2-layer rock-armoured rubble mound seawall with slopes of 1:1.5 and 1:2. The crest level was fixed (560 mm with respect to the bottom of the flume) in all tests. The armour ($D_{n50} = 38$ mm) and filter ($D_{n50} = 17$ mm) materials, each with a minimum thickness of $2D_{n50}$, were sourced from local quarries. The impermeable core of the structure was constructed using 17 mm plywood timber, and the surface friction was enhanced with sand and glue. A smooth acrylic sheet, measuring 500 mm in length, was placed horizontally on the crest of the structure. To prevent leakage of overtopping flow, the sides of the crest at the flume's walls were sealed. During the tests, there were no notable deviations in the trajectories of the overtopping waves, and the presence of wave gauges did not affect the flow of water over the smooth crest.

To measure the overtopping layer thickness on the crest of the structure, two wave gauges were installed at the seaward edge and the middle of the crest (see Fig. 2). A rectangular box was placed beneath the crest to partially submerge the wave gauges. The wave gauges were inserted through holes on the crest into the box, with a submergence depth of 100 mm. To ensure the box remained filled with water throughout the experiments and to minimise the effect of overtopping flows passing over the crest on the water level inside the box, the largest possible size (10 L) was chosen, and the water level was regularly checked. The signals from the probes were recorded and synchronized at a frequency of 20 Hz using a custom MATLAB script. To facilitate better monitoring of the experiments and ensure quality control during the data processing stage, two high-speed cameras were positioned above and beside the seawall.

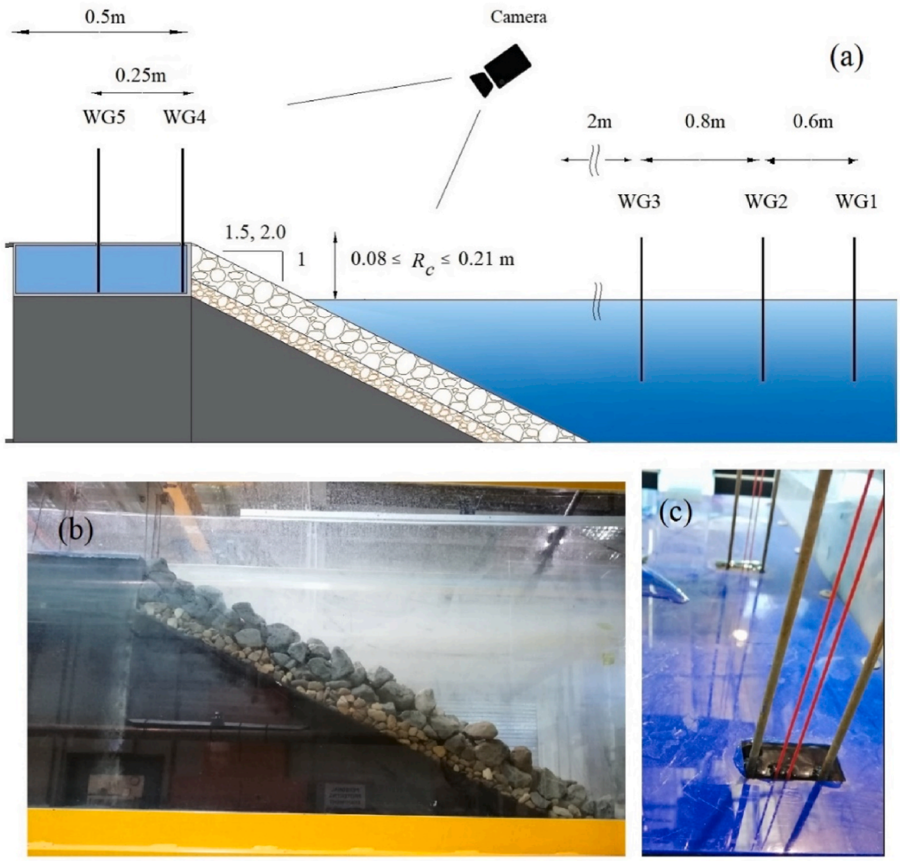

Fig. 2. (a) and (b): Cross section of the model; (c): Wave gauges on the crest of the structure.

3.1. Test programme

A total of 125 tests were conducted on the rubble mound seawall. For each test, 1 000 irregular waves were generated using a JONSWAP spectrum with a peak enhancement factor of $\gamma = 3.3$.

For each structure slope (1:1.5 and 1:2), a series of tests were performed with various still water levels resulting in crest freeboards $R_c =$ 0.08, 0.10, 0.12, 0.13, 0.14, 0.16, 0.18 and 0.21 m. For each crest freeboard, different wave heights (H_{m0}), from 0.07m to 0.13m with an increment of 0.01 m, were combined with different wave periods. Consequently, the wave steepness $s_{m-1,0}$ varied between 0.015 and 0.057. The ranges of the key overtopping parameters in the present study are provided in Table 2. A practical range of the relative crest freeboard ($0.75 \leq R_c/\ H_{m0} \leq 2.36$) was also selected. All tests were conducted in deep water ($h/H_{m0} > 3$) and under non-breaking (surging) wave ($Ir_{m\text{-}1,0} > 1.8$) conditions.

Table 2
The ranges of key parameters for the present study.

Parameter	Range
R_c (m)	0.08–0.21
H_{m0} (m)	0.07–0.13
$T_{m-1,0}$ (s)	1.07–1.96
h (m)	0.35–0.48
$R_c/\ H_{m0}$	0.75–2.36
$tan\ \alpha$	0.5–0.66
$s_{m-1,0}$	0.015–0.057
$Ir_{m\text{-}1,0}$	2.15–5.33
$h/\ H_{m0}$	3.20–6.66

4. Data processing

The thickness of the wave overtopping flow was measured at the seaward edge and the middle of the crest using two wave gauges. These wave gauges recorded a continuous time series of flow thickness on the crest. To accurately calculate the overtopping flow thickness, the recorded raw signals underwent the following processing steps:

First, overtopping events were identified using a threshold-down-crossing algorithm in the time domain. A fixed threshold value (r_s) was selected for each signal. The optimal threshold value depends on various factors such as the nature of the signal (including structural features), incident wave conditions, and the probe's location. If the threshold value (r_s) is set too high, overtopping events with thickness below the threshold will go undetected. Conversely, setting the threshold value too low may result in the base noise of the signal affecting the analysis and leading to misleading results (refer to Fig. 3).

Due to the turbulent nature of overtopping flow and water splash, especially at the seaward edge of the crest, wave gauges may produce unrealistic overtopping events. To address this issue, the coupling method proposed by Formentin and Zanuttigh (2019) was employed. This method is based on the assumption that each overtopping event should be detected by both probes installed on the crest, with a delay dependent on the distance between the probes and the wave celerity. In other words, when one probe detects an individual overtopping event, its corresponding pair should be detected by the second probe within an acceptable delay range. [dt_{min}, dt_{max}]:

$$dt\_(min) = \max\left(\frac{d_w}{c_d}, \frac{1}{S_f}\right) \tag{11}$$

$$dt\_(max) = \frac{d_w}{c_s} \tag{12}$$

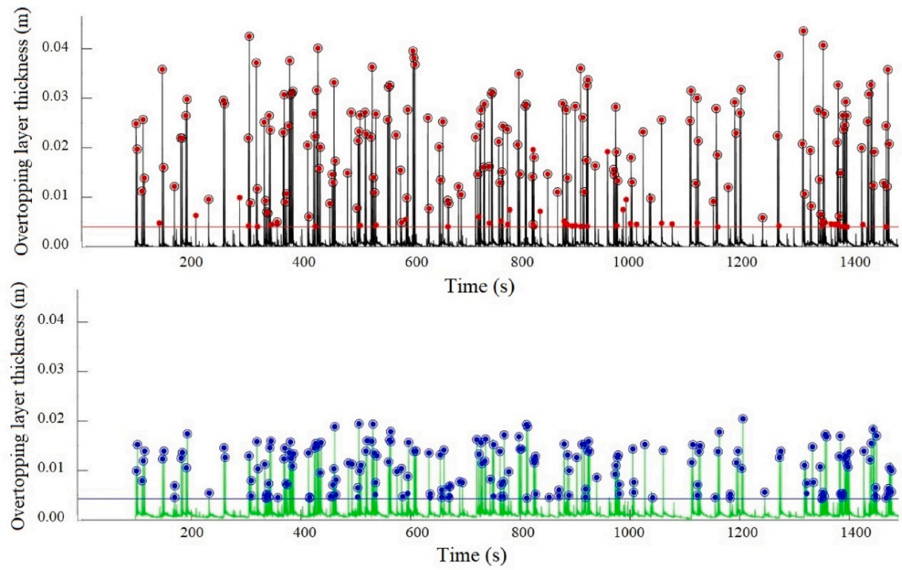

Fig. 3. Recorded wave overtopping layer thickness at the seaward edge (top) and the middle (bottom) of the crest (Each circle corresponds to the detection of an individual overtopping event and horizontal lines show down-crossing threshold). $H_{m0} = 0.1\ m$, $T_p = 1\ s$.

where d_w is the distance between two probes, c_d is the maximum wave celerity (L_{op}/T_p), and S_f is the sampling rate. The minimum celerity in shallow water (c_s) is computed based on the minimum value of the measured flow thickness at the first wave gauge (h_{1min}) as $\sqrt{gh_{1\ min}}$ (Formentin and Zanuttigh, 2019). If the recorded time delay falls outside the acceptable range, the paired overtopping events are discarded. Fig. 3 illustrates the recorded signals of overtopping layer thickness using two wave gauges on the crest, along with the identification of overtopping events using a threshold-down-crossing algorithm for a typical test with $H_{m0} = 0.1$ m, $T_p = 1.90$ s, $h = 0.43$ m. Although the developed computer code could determine the overtopping layer thickness using the recorded signals, video recordings (side view) were also visually inspected to ensure the accuracy of the data during quality control. For further details regarding the challenges and complexities of analysing such signals, readers are referred to Formentin and Zanuttigh (2019), and Koosheh et al. (2021).

5. Results and discussions

As discussed in Section 2, the overtopping layer thickness on the crest of the structure can be correlated with the difference between the wave run-up elevation exceeded by 2% of the incident waves and the crest freeboard. The skill metrics, Normalized Bias (NBIAS), and Scatter Index (SI), were utilized to quantify the performance of the formulas in estimating the overtopping layer thickness:

$$NBIAS = \frac{1}{E_{m,av}}\left(\frac{1}{n}\sum_{i=1}^{n}\left[E_{e,i} - E_{m,i}\right]\right) \times 100 \tag{13}$$

$$SI = \frac{1}{E_{m,av}}\sqrt{\frac{1}{n}\sum_{i=1}^{n}\left\{\left[E_{e,i} - E_{m,i}\right]^2\right\}} \times 100 \tag{14}$$

where $E_{e,i}$ and $E_{m,i}$ are the estimated and measured values, respectively, $E_{m,av}$ is the average of measured values, and n stands for the number of records.

5.1. Overtopping layer thickness at the seaward edge of the crest

Table 3 compares the performance of existing empirical formulas in estimating the wave overtopping layer thickness at the seaward edge of the crest, $h_{A,2\%}(R_c)$ for rubble mound seawalls. In practical design scenarios, wave run-up values are not readily available and need to be estimated. Therefore, the original wave run-up formulas suggested by the respective authors were used, as indicated in Table 3. The roughness factor of $\gamma_f = 0.55$, proposed by EurOtop (2018) for rough structures (2-layer rocks) with an impermeable core, was employed to estimate the wave run-up. The overtopping layer thickness, $h_{A,2\%}(R_c)$, was estimated using Eq. (1) for van Gent (2002) formula ($\gamma_f = 0.55$) and Eq. (6) for EurOtop (2018) and Mares-Nasarre et al. (2019) formulas. The formulas developed for dikes underestimated the dimensionless overtopping layer thickness at the seaward edge, $h_{A,2\%}(R_c)/H_{m0}$ where EurOtop (2018) formula with $NBIAS = -55\%$ and $SI = 62\%$ performed slightly better than that of van Gent (2002) with $NBIAS = -63\%$ and $SI = 69\%$. The formula proposed by Mares-Nasarre et al. (2019), specifically developed for rubble mound breakwaters with a permeable core, demonstrated significantly better performance than the formulas developed for dikes, with an *NBIAS* of 20% and an *SI* of 39%. However, it should be noted that overall, the existing formulas yield biased estimation of the overtopping layer thickness at the seaward edge of rubble mound seawalls.

Table 3
Accuracy metrics of estimation of $h_{A,2\%}$ $(R_c)/H_{m0}$ using different formulas.

Formula	$h_{A,2\%}$ $(R_c)/H_{m0}$ estimator	$R_{u2\%}$ estimator ($\gamma_f = 0.55$)	*NBIAS* (%)	*SI* (%)	Structure type
van Gent (2002)	Eq. 1	Eq. 3	−63	69	Dike (smooth slope and crest, impermeable)
EurOtop (2018)	Eq. 6	Eq. 9	−55	62	Dike (smooth slope and crest, impermeable)
Mares-Nasarre et al. (2019)	Eq. 6	Eq. 9	20	39	Breakwater (rough slope and crest, permeable)
Present study ($c^*_{A,h} = 0.24$)	Eq. 1	Eq. 9	0	27	Seawall (smooth crest, rough slope, impermeable)

Fig. 4 shows the scatter plots of dimensionless difference between $R_{u2\%}$ and R_c against dimensionless overtopping layer thickness at the seaward edge of the crest $h_{A,2\%}(R_c)/H_{m0}$ for different structure slopes. This figure indicates that, within the range of tested slopes, the

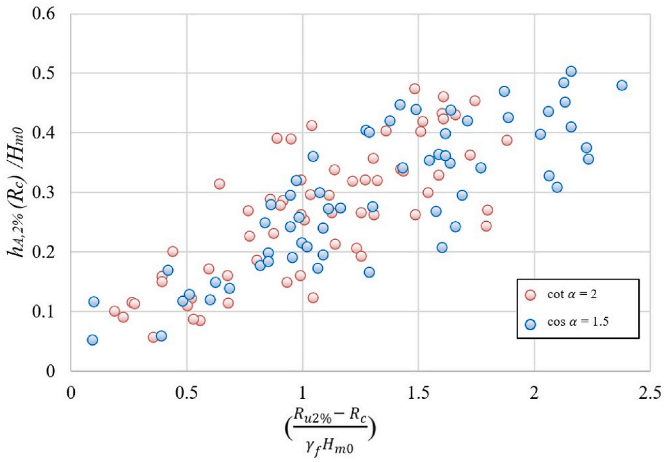

Fig. 4. Dimensionless difference between R_{u2}% and the crest free board against measured $h_{A,2\%}(R_c)/H_{m0}$ for different slopes of the structure.

coefficient $c^*_{A,h}$, in Eq. (1) does not depend on the slope angle. To obtain a formula with an improved level of performance in estimating the overtopping layer thickness on the crest of the present study case namely rubble mound seawall, an optimal value of $c^*_{A,h} = 0.24$ was obtained using bias correction of Eq. (1). The $R_{u2\%}$ values were estimated using Eq. (9) and $\gamma_f = 0.55$.

The proposed coefficient of $c^*_{A,h} = 0.24$ in this study rubble mound seawalls with an impermeable core is about 37% higher than that of van Gent (2002)'s (refer to Table 1) coefficient proposed for dikes (smooth, impermeable core). Apart from different validity ranges of the present study and van Gent (2002) in terms of seawall slope, the difference in obtained $c^*_{A,h}$ values can be explained by difference in their structural features such as slope roughness.

By using the proposed coefficient, the scatter index (SI) of the estimation of $h_{A,2\%}(R_c)/H_{m0}$ was reduced to 27% with 12% and 35% improvement compared to Mares-Nasarre et al. (2019) and EurOtop (2018) formulas, respectively. The scatter plot of measured against estimated values of $h_{A,2\%}(R_c)/H_{m0}$ using the existing formulas and the newly proposed one are shown in Fig. 5. It should be mentioned that as Eq. (3), the run-up formula of van Gent (2002), leads to some negative values of $R_{u2\%} - R_c$, some data points with negative estimations are not seen in the plot.

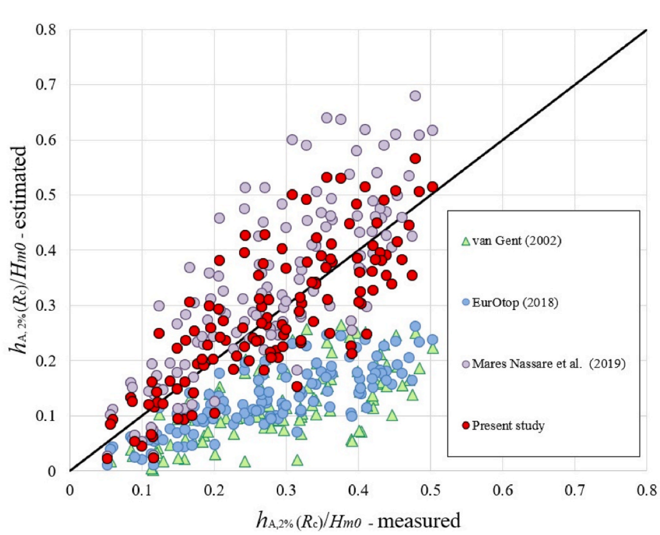

Fig. 5. Estimated vs measured $h_{A,2\%}$ $(R_c)/H_{m0}$ ($\gamma_f = 0.55$), using existing formulas for dikes and rubble mound breakwaters, and newly proposed one for rock-armoured seawall.

5.2. Overtopping layer thickness midway along the crest

The overtopping flow exhibits its maximum thickness at the seaward edge of the crest, and as it progresses landward, the thickness gradually decreases due to energy dissipation. The performance of the existing formulas in estimating the overtopping layer thickness at the middle of the crest, $h_{c,2\%}(x_c = G_c/2)/H_{m0}$, is provided in Table 4. Here, Eq. (2) was used for van Gent (2002) and Mares-Nasarre et al. (2019) formulas, while, for EurOtop (2018) formula, estimated values were calculated using Eq. (8). Wave run-up ($\gamma_f = 0.55$) was estimated using the original formulas proposed by the authors (see Table 4) and the estimated values of and $h_{A,2\%}(R_c)/H_{m0}$ were obtained as discussed above.

As seen, the existing formulas, developed for dikes, underestimated $h_{c,2\%}(x_c = G_c/2)/H_{m0}$ where $NBIAS = -20\%$ and $NBIAS = -21\%$ were recorded for van Gent (2002) and EurOtop (2018) formulas, respectively. In terms of the *SI* metric, the EurOtop (2018) formula with $SI =$ 26% slightly performed better than van Gent (2002) formula. Consistent with $h_{A,2\%}(R_c)/H_{m0}$, the formula proposed by Mares-Nasarre et al. (2019) overestimated $h_{c,2\%}(x_c = G_c/2)/H_{m0}$ with $NBIAS = 26\%$ and $SI =$ 35%.

For the present study case, considering a smooth and impermeable crest, it is reasonable to assume an exponential spatial distribution, as given by Eq. (2) proposed for dikes. However, since the overtopping layer thickness has only been measured at two points along the crest, namely the seaward edge and the middle, the coefficient $c^*_{c,h}$ cannot be calibrated. Hence, following EurOtop (2018), it was assumed that overtopping layer thickness remains almost constant along the crest after an initial turbulent zone. The correlation between the measured $h_{A,2\%}(R_c)/H_{m0}$ and $h_{c,2\%}(x_c = G_c/2)/H_{m0}$ was investigated. As shown in Fig. 6, the best fit line shows that the overtopping layer thickness at the middle of the crest, $h_{c,2\%}(x_c = G_c/2)/H_{m0}$, is well correlated and is approximately half the thickness at the seaward edge $h_{A,2\%}(R_c)/H_{m0}$ (i.e. $h_{c,2\%}(x_c = G_c/2)/H_{m0} = \frac{1}{2}\ h_{A,2\%}(R_c)/H_{m0}$). This means overtopping thickness at the middle point is slightly less than EurOtop (2018) suggestion ($=\frac{2}{3}$; $h_{A,2\%}R_c/H_{m0}$) for dikes. Fig. 6 also shows that, within the range of tested slopes, the correlation between the layer thickness at the start of the crest and at the middle of the crest does not depend on the slope angle. The scatter plot of measured against estimated $h_{c,2\%}(x_c = G_c/2)/H_{m0}$ using the existing formulas, and the proposed one in the present study is shown in Fig. 7.

The accuracy of a good model should be independent of the governing parameters value. To assess this, Discrepancy Ratio (*DR*) was used. This dimensionless metric is defined as the ratio of the estimated value to the measured one. Fig. 8 plots the DR values of formulas proposed in this study to estimate $h_{A,2\%}(R_c)/H_{m0}$ and $h_{c,2\%}(x_c = G_c/2)/H_{m0}$ against some key dimensionless parameters including the slope of the seawall (*tan α*), wave steepness ($s_{m-1,0}$), Iribarren number ($Ir_{m-1,0}$) and

Table 4
Accuracy metrics of estimation of $h_{c,2\%}$ $(x_c = G_c/2)/H_{m0}$ using different formulas.

Formula	$R_{u2\%}$ estimator (γ_f = 0.55)	NBIAS (%)	SI (%)	Structure type
van Gent (2002)	Eq. 3	−20	29	Dike (smooth slope and crest, impermeable)
EurOtop (2018)	Eq. 9	−21	26	Dike (smooth slope and crest, impermeable)
Mares-Nasarre et al. (2019)	Eq. 9	26	35	Breakwater (rough slope and crest, permeable)
Present study	Eq. 9	0	16	Seawall (smooth crest, rough slope, impermeable)

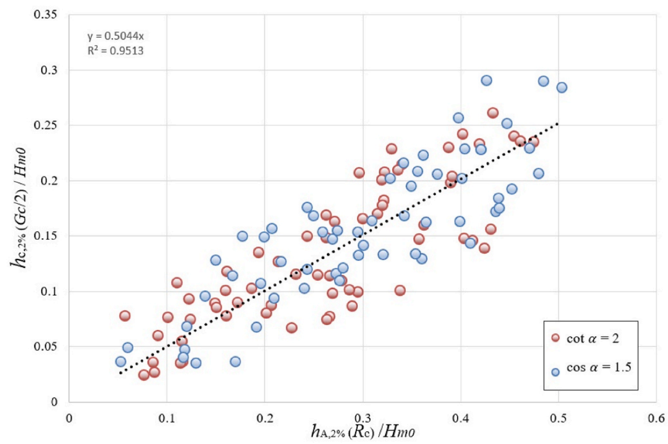

Fig. 6. Measured $h_{A,2\%}(R_c)/H_{m0}$ against $h_{c,2\%}$ $(x_c = G_c/2)/H_{m0}$.

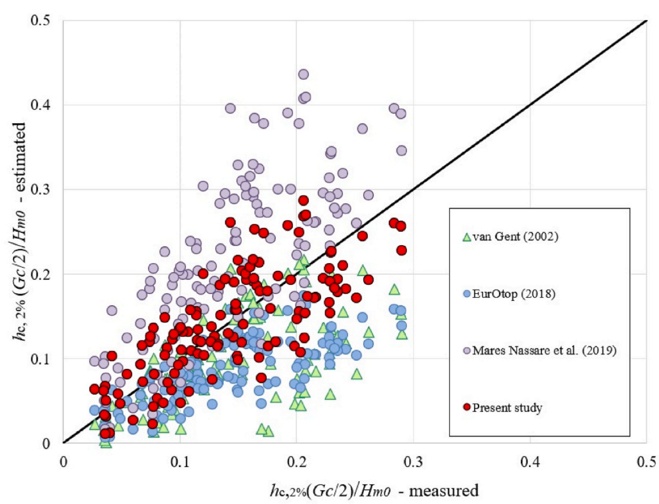

Fig. 7. Measured vs estimated $h_{c,2\%}$ $(x_c = G_c/2)/H_{m0}$ using existing formulas for dikes and rubble mound breakwaters, and newly proposed one (present study) for rock-armoured seawall.

$(R_{u2\%}$ - $R_c)/\gamma_f$ H_{m0}. The distribution of data points is almost symmetric around $DR = 1$ line and no discernible trend can be observed. This indicates that the proposed formulas have been optimally trained with minimum systematic error. The scatter of the estimation decreases by increase of $(R_{u2\%}$ - $R_c)/\gamma_f$ H_{m0}, reflecting the challenges associated with measuring small overtopping events with relatively lower wave run-up levels.

6. Conclusions and recommendations

The safety assessment of coastal structures commonly relies on overtopping parameters such as the mean overtopping rate (q) and the maximum individual overtopping volume (V_{max}). However, it is crucial to also consider the overtopping layer thickness (or flow depth) which is important in assessing overtopping hazard to pedestrians and vehicles located on or behind the crest. This research aimed to gain a better understanding of the overtopping layer thickness on the crest of rubble mound seawalls. To achieve this goal, a total of 125 2D small-scale physical model tests were conducted on a 2-layer rock armoured seawall featuring an impermeable core with armour slopes of 1:1.5 and 1:2. The overtopping layer thickness was measured at both the seaward edge and the middle of the crest using two wave gauges.

Wave overtopping layer thickness on the crest of coastal structures is a spatially and temporally variable phenomenon that is historically related to wave run-up on the seaward slopes and the crest freeboard of the structure. However, existing empirical formulas, originally developed for dikes (i.e., van Gent, 2002; EurOtop, 2018), underestimated the wave overtopping layer thickness on the crest of rubble mound seawalls. On the other hand, the formula developed by Mares-Nasarre et al. (2019) for rubble mound breakwaters slightly overestimated the overtopping layer thickness both at the edge and the middle of the seawall's crest. This difference can be attributed to variations in the structural characteristics between existing studies (dikes or breakwaters) and rubble mound seawalls. Dikes typically exhibit smoother and gentler slopes than seawalls, resulting in different interactions between waves and the structure compared to rubble mound seawalls with rough surfaces. Similarly, formulas tailored for breakwaters with rough surfaces and a permeable core cannot be used for seawalls because of their impermeable cores.

Eq. (1) was adapted to the study case by correcting the estimation bias, and $c^*_{A,h} = 0.24$ was proposed. The calibrated coefficient leads to a better estimation of dimensionless overtopping layer thickness at the seaward edge ($h_{A,2\%}(R_c)/H_{m0}$) of rubble mound seawalls, with $SI = 27\%$. This improvement represents a 35% and 10% enhancement compared to EurOtop (2018) and Mares-Nasarre et al. (2019) formulas, respectively. Subsequently, following EurOtop (2018), by assuming abrupt drop immediately behind the crest edge and then a constant thickness of the overtopping layer over the crest of the structure, the correlation between the overtopping layer thickness at the middle of the crest, $h_{c,2\%}(x_c = G_c/2)$, and at the seaward edge $h_{A,2\%}(R_c)$ was investigated. A suggestion was made that $h_{c,2\%}(x_c = G_c/2)/H_{m0}$ can be approximated by $\frac{1}{2}h_{A,2\%}(R_c)/H_{m0}$. This resulted in improvements of 10% and 19% for the estimation of $h_{c,2\%}(x_c = G_c/2)$ compared to those of EurOtop (2018) (developed for dikes, i.e. smooth and impermeable structures), and Mares-Nasarre et al. (2019) formula (developed for rubble mound breakwaters with a rough slope and permeable core), respectively. For the overtopping layer thickness at the crest, the roughness and permeability of the surface can also play a significant role in the spatial distribution of overtopping flow and how it evolves toward the lee side. The results provided for the overtopping layer thickness on the crest of the seawall in the present study are based on a smooth and impermeable crest. However, in the case of rubble mound seawalls with a rough and permeable crest (covered by armour units), where overtopped water percolates through the armour units placed in the crest, the suggested ratio of $h_{c,2\%}(x_c = G_c/2)/H_{m0}$ to $h_{A,2\%}(R_c)/H_{m0}$ may be somewhat different. For an example of wave overtopping layer thickness estimation at the seaward edge and middle of the crest of a real rubble mound seawall using both existing formulas and the proposed one from the present study, readers are referred to the appendix.

In this research, relatively steep slopes of the seawall under non-breaking wave conditions at the foreshore were tested. For future studies, it is recommended to verify whether the results can be generalized to gentler slopes and shallow foreshores as well. Additionally, it should be noted that the measurements of overtopping layer thickness were taken only at two points on the crest, specifically at the seaward edge and middle. Hence, following EurOtop (2018), a constant thickness was assumed after an abrupt decrease at the edge. To better investigate variations in overtopping layer thickness along the crest of the seawall, multiple measurements are recommended. In this way, findings will become more robust and applicable to a wider range of conditions which will provide valuable insights for coastal protection strategies.

CRediT authorship contribution statement

Ali Koosheh: Conceptualization, Methodology, Formal analysis, Investigation, Data curation, Writing – original draft, Visualization. **Amir Etemad-Shahidi:** Conceptualization, Methodology, Formal analysis, Supervision, Writing – review & editing. **Nick Cartwright:**

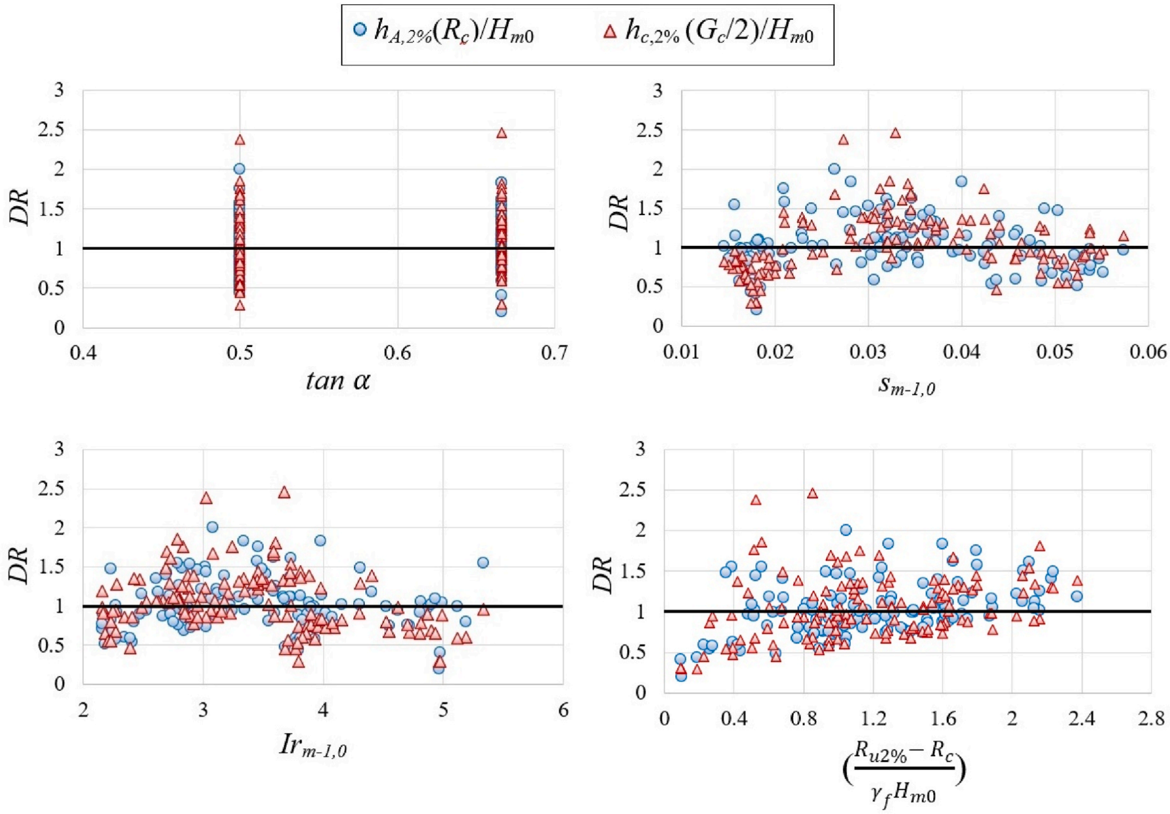

Fig. 8. Discrepancy ratios of estimated $h_{A,2\%}(R_c)/H_{m0}$ and $h_{c,2\%}$ $(x_c = G_c/2)/H_{m0}$ of the proposed formulas against seaward slope of structure (top-left); wave steepness (top-right), Iribarren number (bottom-left) and dimensionless difference of wave run-up and the crest freeboard.

Conceptualization, Supervision, Writing – review & editing. **Rodger Tomlinson:** Conceptualization, Supervision, Writing – review & editing. **Marcel R.A. van Gent:** Conceptualization, Supervision, Writing – review & editing.

Declaration of competing interest

We wish to confirm that there are no known conflicts of interest associated with this publication and there has been no significant financial support for this work that could have influenced its outcome.

We confirm that the manuscript has been read and approved by all named authors and that there are no other persons who satisfied the criteria for authorship but are not listed. We further confirm that the order of authors listed in the manuscript has been approved by all of us.

We confirm that we have given due consideration to the protection of intellectual property associated with this work and that there are no impediments to publication, including the timing of publication, with respect to intellectual property. In so doing we confirm that we have followed the regulations of our institutions concerning intellectual property.

We understand that the Corresponding Author is the sole contact for the Editorial process (including Editorial Manager and direct communications with the office). He/she is responsible for communicating with the other authors about progress, submissions of revisions and final approval of proofs. We confirm that we have provided a current, correct email address which is accessible by the Corresponding Author and which has been configured to accept email from ali.koosheh@griffithuni.edu.au

Data availability

The authors do not have permission to share data.

Acknowledgments

The authors would like to acknowledge the financial support from Griffith University. The first author was funded by GUPRS and GUIPRS scholarships.

Glossary

$c^*_{A,h}$	Overtopping flow thickness coefficient at the seaward edge of the crest
$c^*_{c,h}$	Overtopping flow thickness coefficient over the crest
c_d	Maximum wave celerity
c_s	Minimum celerity in shallow water
dt_{min}	Minimum lag between the detected events in the coupling process
dt_{max}	Maximum lag between the detected events in the coupling process
d_w	Distance between two wave gauges at the crest of structure in the direction of flow
D_{n50}	Nominal rock diameter
G_c	Crest width

g	Acceleration due to gravity
H	Water depth at the toe of the structure
h_{1min}	Minimum measure thickness at the crest edge
$h_{A,2\%}$	Overtopping flow thickness at the seaward crest edge
$h_{c,2\%}$	Overtopping flow thickness over the crest
H_{m0}	Spectral significant wave height
$L_{m-1,0}$	Deep water wavelength estimated as $1.56T^2_{m\text{-}1,0}$
L_{op}	Deep water wavelength based on peak wave period
$R_{u2\%}$	Run-up level exceeded by the 2% of the incident waves
R_c	Crest Freeboard
S_f	Sampling frequency
$s_{m-1,0}$	Spectral wave steepness
$T_{m\text{-}1,0}$	Spectral wave period
T_p	Peak wave period
x_c	Position on the crest with respect to the seaward edge
γ_f	Roughness factor
$\gamma_{f\ surging}$	Modified roughness factor
γ_β	Oblique wave factor
$Ir_{m\text{-}1,0}$	Iribarren number

Appendix

As an example, overtopping layer thickness is estimated for a real rubble mound seawall. The design conditions are:
$H_{m0} = 3.0$ m, $T_p = 11.1$ s $T_m = 9.7$ s, $T_{m\text{-}1,0} = 10.1$ s, $h = 9.9$ m, rock two-layer, impermeable core, $\gamma_f = 0.55$, cot $\alpha = 1.75$, $R_c = 5.08$ m.

a) Present study:

$$L_{m\text{-}1,0} = g/2\pi\ T^2_{m\text{-}1,0} = 1.56 \times 10.1^2 = 159.3 \text{ m}$$

$$s_{m\text{-}1,0} = H_{m0} / L_{m\text{-}1,0} = 3.0/159.3 = 0.0188$$

$$Ir_{m\text{-}1,0} = \tan\alpha / \sqrt{s_{m\text{-}1,0}} = 0.57/\sqrt{0.0188} = 4.15$$

$$\gamma_{f\_surging} = \gamma_f + \frac{(Ir_{m-1,0} - 1.8)(1-\gamma_f)}{8.2} = 0.55 + \frac{(4.15-1.8)(1-0.55)}{8.2} = 0.68$$

$$\frac{R_{u2\%}}{H_{m0}} = \min\left(1.65\gamma_f\gamma_\beta Ir_{m-1,0},\ 1.0\ \gamma_{f\_surging}\gamma_\beta\left(4 - \frac{1.5}{\sqrt{Ir_{m-1,0}}}\right), 3\right) = 2.21$$

$$R_{u2\%} = 2.21 \times 3 = 6.63 \text{ m}$$

$$\frac{h_{A,2\%}(R_c)}{H_{m0}} = c^*_{A,h}\left(\frac{R_{u2\%} - R_c}{\gamma_f H_{m0}}\right) = 0.24\left(\frac{6.63 - 5.08}{0.55 \times 3}\right) = 0.225$$

$$h_{A,2\%}(R_c) = 0.225 \times 3 = 0.67 \text{ m}$$

$$h_{c,2\%}(x_c = G_c/2) = \frac{1}{2} \times 0.67 = 0.33 \text{ m}$$

b) Van Gent (2002).

$$p = 0.5\frac{c_1}{c_0} = 0.5\frac{3.8}{1.45} = 1.31 < Ir_{m-1,0} = 4.15$$

$$c_2 = 0.25\frac{c_1^2}{c_0} = 0.25\frac{3.8^2}{1.45} = 2.49$$

$$\frac{R_{u2\%}}{\gamma_f H_{m0}} = c_1 - \frac{c_2}{Ir_{m-1,0}} = 3.2$$

$$R_{u2\%} = 3.2 \times 0.55 \times 3 = 5.28 \text{ m}$$

$$\frac{h_{A,2\%}(R_c)}{H_{m0}} = c^*_{A,h}\left(\frac{R_{u2\%} - R_c}{\gamma_f H_{m0}}\right) = 0.15\left(\frac{5.28 - 5.08}{0.55 \times 3}\right) = 0.018$$

$$h_{A,2\%}(R_c) = 0.018 \times 3 = 0.055 \text{ m}$$

$$h_{c,2\%}(x_c = G_c/2) = h_{A,2\%}(R_c).\,exp\left(-c^*_{c,h}\frac{x_c}{G_c}\right) = 0.055\times\ exp\left(-0.4\times\frac{1}{2}\right) = 0.045\text{ m}$$

c) EurOtop (2018).

$$R_{u2\%} = 2.21\ \times\ 3 = 6.63\text{ m (calculated above)}$$

$$\frac{h_{A,2\%}(R_c)}{H_{m0}} = c^*_{A,h}\left(\frac{R_{u2\%} - R_c}{H_{m0}}\right) = 0.2\left(\frac{6.63 - 5.08}{3}\right) = 0.10$$

$$h_{A,2\%}(R_c) = 0.1\ \times 3 = 0.3\text{ m}$$

$$h_{c,2\%}(x_c = G_c/2) = \frac{2}{3}\times\ 0.3 = 0.2\text{ m}$$

d) Mares-Nasarre et al. (2019)

$$R_{u2\%} = 2.21\ \times\ 3 = 6.63\text{ m (calculated above)}$$

$$\frac{h_{A,2\%}(R_c)}{H_{m0}} = c^*_{A,h}\left(\frac{R_{u2\%} - R_c}{H_{m0}}\right) = 0.52\left(\frac{6.63 - 5.08}{3}\right) = 0.27$$

$$h_{A,2\%}(R_c) = 0.27\ \times 3 = 0.81\text{ m}$$

$$h_{c,2\%}(x_c = G_c/2) = h_{A,2\%}(R_c).\exp\left(-c^*_{c,h}\frac{x_c}{G_c}\right) = 0.81\times\ exp\left(-0.89\times\frac{1}{2}\right) = 0.51\text{ m}$$

Table A1
Estimation of overtopping layer thickness on the crest of a real seawall using different formulas

Formula	$h_{A,2\%}(R_c)$ (m)	$h_{c,2\%}(x_c = G_c/2)$ (m)
van Gent (2002)	0.055	0.045
EurOtop (2018)	0.30	0.20
Mares-Nasarre et al. (2019)	0.80	0.51
Present study	0.67	0.33

References

Abt, S.R., Wittier, R.J., Taylor, A., Love, D.J., 1989. Human stability in A high flood hazard zone 1. JAWRA J. Am. Water Resour. Assoc. 25, 881–890.

Allsop, W., Bruce, T., Pearson, J., Alderson, J., Pullen, T., 2003. Violent wave overtopping at the coast, when are we safe?. In: International Conference on Coastal Management 2003, pp. 54–69.

Arrighi, C., Oumeraci, H., Castelli, F., 2017. Hydrodynamics of pedestrians' instability in floodwaters. Hydrol. Earth Syst. Sci. 21, 515–531.

Bae, H.U., Yoon, J.Y., Yun, K.M., Lim, N.H., 2016. Human stability with respect to overtopping flow on the breakwater. Int. J. Appl. Eng. Res. 11, 111–119.

Bosman, G., 2007. Velocity and Flow Depth Variations during Wave Overtopping, Master Thesis. TU Delft.

Cao, D., Yuan, J., Chen, H., Zhao, K., Liu, P.L.-F., 2021. Wave overtopping flow striking a human body on the crest of an impermeable sloped seawall. Part I: physical modeling. Coast. Eng. 167, 103891.

Chen, W., Warmink, J.J., van Gent, M.R.A., Hulscher, S.J.M.H., 2022. Numerical investigation of the effects of roughness, a berm and oblique waves on wave overtopping processes at dikes. Appl. Ocean Res. 118 https://doi.org/10.1016/j.apor.2021.102971. Elsevier.

Cox, J.C., Machemehl, J., 1986. Overload bore propagation due to an overtopping wave. J. Waterw. Port, Coast. Ocean Eng. 112, 161–163.

Endoh, K., Takahashi, S., 1994. Numerically modeling personnel danger on a promenade breakwater due to overtopping waves. In: Coastal Engineering 1994, pp. 1016–1029. Chicago.

Etemad-Shahidi, A., Koosheh, A., van Gent, M.R.A., 2022. On the mean overtopping rate of rubble mound structures. Coast. Eng. 104150.

EurOtop, 2018. In: van der Meer, J.W., Allsop, N.W.H., Bruce, T., de Rouck, J., Kortenhaus, A., Pullen, T., Schüttrumpf, H., Troch, P., Zanuttigh, B. (Eds.), Manual on Wave Overtopping of Sea Defences and Related Structures. www.overtopping-manual.com.

Formentin, S.M., Zanuttigh, B., 2019. Semi-automatic detection of the overtopping waves and reconstruction of the overtopping flow characteristics at coastal structures. Coast. Eng. 152, 103533 https://doi.org/10.1016/j.coastaleng.2019.103533.

Foster, D.N., Cox, R., 1973. Stability of Children on Roads Used as Floodways: Preliminary Study. University of New South Wales, Water Research Laboratory.

Jafari, E., Etemad-Shahidi, A., 2011. Derivation of a new model for prediction of wave overtopping at rubble mound structures. J. Waterw. Port, Coast. Ocean Eng. 138, 42–52. https://doi.org/10.1061/(ASCE)WW.1943-5460.0000099.

Jonkman, S.N., Penning-Rowsell, E., 2008. Human instability in flood flows 1. JAWRA J. Am. Water Resour. Assoc. 44, 1208–1218.

Koosheh, A., Etemad-Shahidi, A., Cartwright, N., Tomlinson, R., Hosseinzadeh, S., 2020. The comparison of empirical formulae for the prediction of mean wave overtopping rate at armored sloped structures. Coast. Eng. Proc. 36, 22-22.

Koosheh, A., Etemad-Shahidi, A., Cartwright, N., Tomlinson, R., van Gent, M.R.A., 2022a. Experimental study of wave overtopping at rubble mound seawalls. Coast. Eng., 104062

Koosheh, A., Etemad-Shahidi, A., Cartwright, N., Tomlinson, R., van Gent, M.R.A., 2022b. Distribution of individual wave overtopping volumes at rubble mound seawalls. Coast. Eng., 104173

Koosheh, A., Etemad-Shahidi, A., Cartwright, N., Tomlinson, R., van Gent, M.R.A., 2021. Individual wave overtopping at coastal structures: a critical review and the existing challenges. Appl. Ocean Res. 106, 102476.

Mansard, E.P.D., Funke, E.R., 1980. The measurement of incident and reflected spectra using a least squares method. In: Coastal Engineering 1980, pp. 154–172.

Mares-Nasarre, P., Argente, G., Gómez-Martín, M.E., Medina, J.R., 2019. Overtopping layer thickness and overtopping flow velocity on mound breakwaters. Coast. Eng. 154, 103561 https://doi.org/10.1016/j.coastaleng.2019.103561.

Mares-Nasarre, P., Molines, J., Gómez-Martin, M.E., Medina, J.R., 2020. Individual wave overtopping volumes on mound breakwaters in breaking wave conditions and gentle sea bottoms. Coast. Eng., 103703

Nørgaard, J.Q.H., Andersen, T.L., Burcharth, H.F., Steendam, G.J., 2013. Analysis of overtopping flow on sea dikes in oblique and short-crested waves. Coast. Eng. 76, 43–54.

Sandoval, C., Bruce, T., 2017. Wave overtopping hazard to pedestrians: video evidence from real accidents. In: Coasts, Marine Structures and Breakwaters 2017: Realising the Potential. ICE Publishing, pp. 501–512.
Schüttrumpf, H., 2001. Wellenüberlaufströmung an Seedeichen: Experimentelle und theoretische Untersuchungen. PhD Thesis. Technical University of Braunschweig.
Schüttrumpf, H., van Gent, M.R.A., 2003. Wave overtopping at seadikes. In: Coast. Struct. 2003 - Proc. Conf, vol. 40733, pp. 431–443. https://doi.org/10.1061/40733(147)36.
Takahashi, S., Endoh, K., Muro, Z.I., 1992. Experimental study on people's safety against overtopping waves on breakwaters. Rep. Port Harb. Inst. 34, 4–31.
TAW, 2002. Technical Report Wave Run-Up and Wave Overtopping at Dikes, Technical Advisory Committee on Flood Defence. TAW, Delft.
Van der Meer, J., Bruce, T., 2014. New physical insights and design formulas on wave overtopping at sloping and vertical structures. J. Waterw. Port, Coast. Ocean Eng. 140, 1–18. https://doi.org/10.1061/(ASCE)WW.1943-5460.0000221.
Van der Meer, J.W., Hardeman, B., Steendam, G.-J., Schüttrumpf, H., Verheij, H., 2010. Flow depths and velocities at crest and landward slope of a dike, in theory and with the wave overtopping simulator. Coast. Eng. Proc. 1 (32), 10. Chicago.
Van der Meer, J.W., Janssen, J., 1994. Wave Run-Up and Wave Overtopping at Dikes and Revetments. VdM VML EB MT2. Delft Hydraulics, publication no. 485.
Van Gent, M.R.A., 2002. Low-exceedance Wave Overtopping Events: Measurements of Velocities and the Thickness of Water-Layers on the Crest and Inner Slope of Dikes. Delft Cluster, Dc030202/H3803.
Van Gent, M.R.A., van den Boogaard, H.F.P., Pozueta, B., Medina, J.R., 2007. Neural network modelling of wave overtopping at coastal structures. Coast. Eng. 54, 586–593.
Zanuttigh, B., van der Meer, J., Bruce, T., Hughes, S., 2013. Statistical characterisation of extreme overtopping wave volumes. Coasts, Mar. Struct. Break. 2013 from Sea to Shore - meet. Challenges Sea 1, 442–451. https://doi.org/10.1680/fsts.59757.0442.